ELSEVIER

Chemical Engineering Journal 135S (2008) S138–S146

Chemical Engineering Journal

www.elsevier.com/locate/cej

Modelling of the residence time distribution in micromixers

D. Bošković *, S. Loebbecke

Fraunhofer Institute for Chemical Technology ICT, P.O. Box 1240, 76318 Pfinztal, Germany

Abstract

A technique for the measurement of the residence time distribution (RTD) in microfluidic devices is presented. The measurements were performed by an input–response technique monitoring a dye tracer concentration spectroscopically at the inlet and outlet of a microfluidic device. The measurement setup ensures the interchangeability of microfluidic devices and thus allows characterising of many different devices containing diverse mixing structures and microchannel geometries.

Since the experimental method is based on an external stimulus the measured RTD data show deviations from the actual RTD of the microfluidic device. These deviations are caused by the connected capillaries and their contribution to the overall RTD of the whole system. Therefore, modelling of the RTD is necessary. Two different models were applied in this study. The first one is the well-known axially dispersed plug flow model which is often used for macroscopic reactors. Since this model was developed for plug flow processes, its applicability to the laminar flow regime of microfluidic devices is strongly limited. Therefore, another empirical model was developed and applied in order to consider a wider range of different microstructures and process parameters.

The RTDs of three different micromixers were investigated in a specified range of flow rates and modelled with the empirical model. Based on these results the mixing performance and integral flow behaviour of the different reactors could be analysed and discussed.

Keywords: Residence time distribution; Microreactor; Deconvolution

1. Introduction

Characterisation of the overall flow behaviour of a reactor by means of residence time distribution (RTD) theory provides essential information from the viewpoint of chemical reaction engineering. Knowledge of the RTD enables the exact prediction of yield for first order reactions and allows close estimation for reactions of order other than first. In addition, the general reactor performance and mixing can be evaluated. Since microreactors and micromixers are available in a great variety of geometries using different mixing principles, the selection of a suitable device for a given application becomes more challenging. Among other characteristics (like mixing efficiency) knowledge of the RTD of a certain microfluidic device would be a useful help to identify the most appropriate one.

RTD experiments are usually performed by introducing an input signal (impulse, step, periodic, etc.) with an inert tracer at the inlet of a reactor. By time resolved measurement of the response at the outlet of the reactor the RTD can be obtained.

Even though residence time distribution analysis is widely used for the characterisation of macroscopic reactors, there are no common techniques for microfluidic devices available. Guenther et al. [1] presented a technique where a dye tracer was injected by a T-shaped injection unit and the concentration of the tracer was measured by a special transmittance sensor. The further development of this approach is presented here. Other work described in literature is based on the RTD analysis of custom-made microdevices specially developed for this purpose. Trachsel et al. [2], for example, presented a microdevice with an integrated injection unit and a meandering microchannel. The device was made of PDMS and due to the transparency of this material fluorescence measurements can be carried out. The advantage of this technique is that the input signal can be introduced directly at the beginning of the microstructure. However, this technique is very much limited to this specific device. Microreactors and micromixers are nowadays available in a great variety of materials where in situ measurements are mostly not applicable since the materials that are used for reasons of certain chemical, physical or mechanical properties are often not transparent. Moreover, the available microfluidic devices have very different geometries and mixing structures. Therefore, a universal technique which can be applied to different microreactors and micromixers is desirable. Accordingly the necessary sensors

* Corresponding author. Tel.: +49 721 4640 759; fax: +49 721 4640 111.
E-mail address: db@ict.fhg.de (D. Bošković).

1385-8947/$ – see front matter © 2007 Elsevier B.V. All rights reserved.
doi:10.1016/j.cej.2007.07.058

Nomenclature

$c(t)$	concentration of tracer (mol/L)
d_h	hydraulic diameter
D_{ax}	axial diffusion coefficient (m^2/s)
$E(i\omega)$	Fourier transform of $E(t)$, transfer function
$E(t)$	normalized density distribution function
L	length
M	parameter of empirical model
N	parameter of empirical model
Pe	Peclet number (uL/D_{ax})
Re	Reynolds number
s	skewness
t	time
t_k	defined by Eq. (11)
t_{max}	maximum residence time in empirical model
t_{min}	minimum residence time in empirical model
u	linear velocity (m/s)
$x(t)$	normalized input signal
$y(t)$	normalized response signal
$y_{calc}(t)$	calculated normalized response (by Eq. (3))

Greek symbols

ε	sum of squares of deviation
Θ	normalized time ($\Theta = t/\tau$)
ν	kinematic viscosity (m^2/s)
$\sigma(\Theta)^2$	variance
τ	mean residence time
ω	Fourier transform parameter

and actuators have to be connected externally even though this is accompanied by some drawbacks, which will be discussed later.

2. Experimental

A scheme of the experimental setup is shown in Fig. 1. Although different types of input signals are in principal possible, in this work only impulse experiments were performed since the resulting time distribution density curves are the most common basis for the subsequent data processing and modelling [3].

In order to ensure accurate flow rates with low pulsation a syringe pump (TSE Systems, Bad Homburg, Germany) was used for the feed of the liquids. The pump was equipped with two syringes (Hamilton, Bonaduz, Switzerland), one filled with water, the other with an aqueous solution of the dye Basic Blue 3 (CAS No. 33203-82-63). This dye was used because of its low molecular diffusion coefficient in water (3.78×10^{-6} cm^2/s) [4]. Moreover, in a previous study [5], the applicability of numerous organic dyes was tested and most of them showed considerable affinity to the inner walls of PTFE or PFA capillaries. As a consequence a distinctive tailing of the measured curves is observed. Basic Blue 3 turned out to be the best tracer for the present application since it shows no affinity to PTFE and PFA.

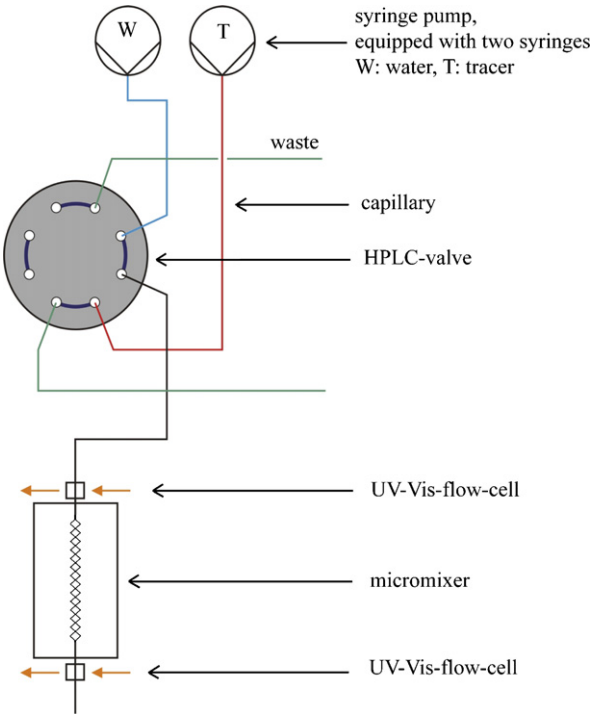

Fig. 1. Scheme of the experimental setup.

The syringes filled with the liquids were connected to a HPLC valve by using standard 1/16 in. HPLC capillaries with an inner diameter of 1/32 in. (0.8 mm). The fast cycling HPLC valve which was used for the introduction of the input signal was driven by a microelectronic valve actuator (Valco Instruments, Houston, USA). The valve can be driven in different modes. By switching once, a step signal and by switching twice an impulse signal can be introduced. By using a valve with an internal sample volume (here 0.2 μL) an impulse experiment can be performed by switching only once. All these different modes were used to verify whether the switching and the accompanied short flow interruption have an influence on the resulting curves. The cycling time to switch from one position to the other (by 45°) was 85 ms. The inline measurement of the concentration was realized by in-house made UV–vis flow-through cells which were directly attached to the inlet and outlet of the micromixer (Fig. 2).

The optical cells were pulled over the capillaries and the concentration of the tracer (mean concentration over the cross section) was measured spectroscopically perpendicular to the flow direction inside of the capillary. Since the optical flow-

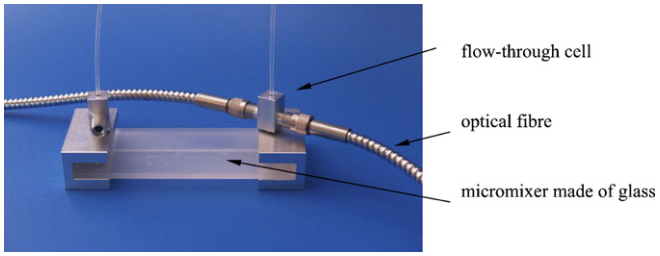

Fig. 2. Micromixer with attached UV–vis flow-through cells.

through cells provide no additional internal volume they have no impact on the flow and no additional contribution to the overall RTD. By using headless HPLC fittings (Upchurch, Oak Harbor, USA) the distance between the optical cells and the micromixer which causes a potential error in the raw RTD data can be minimized to approx. 7 mm. Transparent PFA capillaries were used to improve the spectroscopic signal. Only standard HPLC equipment which is widely used in microreaction technology was used for all connections and therefore many different microfluidic devices can be inserted into the experimental setup. Due to the geometry of the optical cells it is also possible to use capillaries of other diameter which ensures additional flexibility. The optical cells were connected to a two-channel spectrometer (Ocean Optics, Dunedin, USA) by optical fibres. The two separate spectrometer channels were calibrated by the supplier in order to provide equal signals. However, in the present application, minor discrepancies in the measured signals at the two measuring points are possible due to fabrication tolerances of the tailor made flow cells. To avoid this problem all measured curves were normalized prior to further processing. Additionally, the appropriate concentration range of the dye solution was determined to be in the linear Lambert–Beer range. In order to have a defined starting time for the measurement the spectroscopic acquisition was activated by a trigger signal provided by the valve actuator.

2.1. Investigated micromixers

The RTD of three different micromixers was characterised at flow rates ranging from 0.5 to 2.0 mL/min. Depending on the channel geometry of the individual micromixer the Reynolds numbers are ranging from approx. 3 to 80. All investigated micromixers contain mixing structures which can be classified as split-and-recombine structures. The mixing in split-and-recombine mixers is based on a serial multilamination which increases the contact surface and enables shorter diffusion times. In the meantime it is commonly known, that mixing in most of such type of micromixers is additionally enhanced by evolving secondary flow patterns causing chaotic advection and improving radial mixing [6–8].

Pictures and drawings of the investigated micromixers are shown in Fig. 3. The ST-mixer in Fig. 3(a) (Little Things Factory, Ilmenau, Germany) is made of glass by a sandblasting technique. The three-dimensional structure consists of 32 mixing elements which are twisted by 90°. This micromixer has been used for numerous chemical reactions and provides a good mixing performance as it was verified by experimental characterisation methods [9]. The "degree" of multilamination is assumed to be lower than in the other investigated mixers. There are flow-splitting units in the structure, but there are no specific, spatially separated rearrangement elements. Therefore, it is assumed that in this device mixing due to secondary flows and chaotic advection is prevailing.

Fig. 3(b) shows another micromixer that was tested. It consists of 11 parallel channels each containing 7 three-dimensional G-shaped split-and-recombine elements. Due to the definite splitting and rearrangement based on three dimensions, the split-and-recombine character is more distinctive than in the ST-mixer. The inlet and outlet channels are shaped trapezoidal to ensure uniformly distributed flow over the parallel channels [10,11]. The microreactor is made of silicon and the typical channel dimensions are 0.25 mm × 0.25 mm.

The third micromixer which was tested is shown in Fig. 3(c). The so-called Statmix 6 mixer (IPHT, Jena, Germany) was build up of three layers, one silicon layer in the middle with two covers of glass on the top and the bottom. The mixer contains one

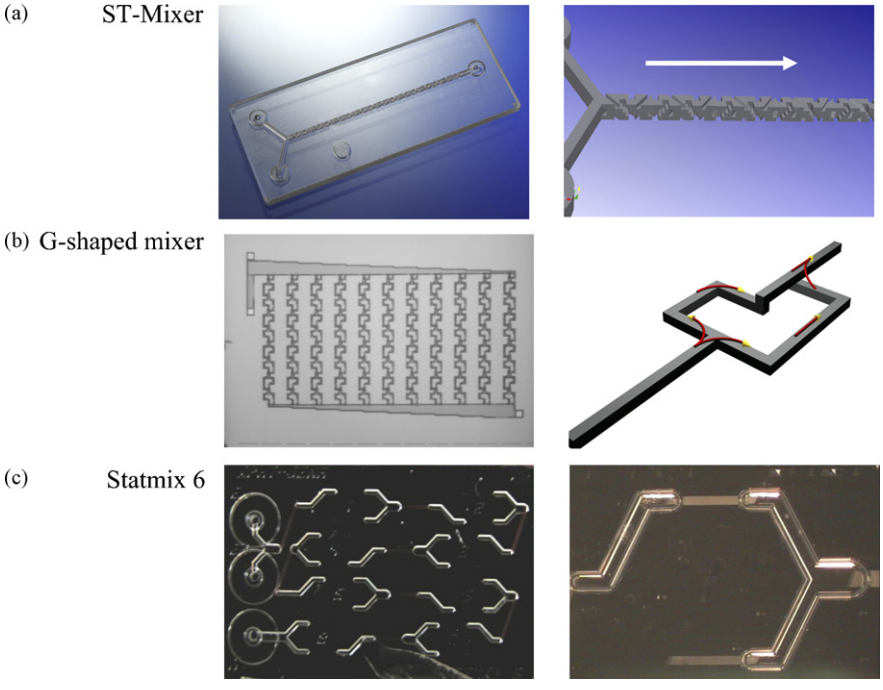

Fig. 3. (a–c) Pictures and details of the channel design of the three micromixers characterised.

channel with eight sequential split-and-recombine elements. The channel widths are ranging from 0.2 to 0.7 mm [12].

All investigated microdevices have two inlet ports and one outlet. In order to ensure the same time-scale for the input- and the response-signal, only one inlet port should be used for RTD measurements. Therefore one inlet was always closed with a plug. To avoid dead volume in the plugged inlet channel the device was filled with water prior to RTD measurements.

2.2. Data preparation

Two spectroscopic curves, one for the inlet and one for the outlet of the micromixer were obtained by the described experimental method. Each curve shows the fraction of fluid at a certain residence time. In order to use the measured curves for modelling, they have to be normalized. The normalized density function as the response to an ideal Dirac delta function is given by

$$E(t) = \frac{c(t)}{\int_0^\infty c(t)\,\mathrm{d}t} \tag{1}$$

and can be calculated for the input and the response signal by numerical integration. The first moment of the distribution which represents the mean residence time can be accordingly calculated by

$$\tau = \int_0^\infty E(t)t\,\mathrm{d}t = \frac{\int_0^\infty c(t)t\,\mathrm{d}t}{\int_0^\infty c(t)\,\mathrm{d}t}. \tag{2}$$

The RTD of a specific micromixer cannot be calculated directly from the measured data. The input signal is introduced in front of the micromixer via a capillary of certain length between the valve and the micromixer. Hence, the signal is not an ideal delta and is further modified while flowing through the capillary towards the inlet of the microfluidic device. Therefore, the measured response comprises both distributions of the periphery and of the micromixer itself. Such a coupled system can be described by the convolution integral which is known from linear system theory:

$$y(t) = \int_0^t x(t-t')E(t')\,\mathrm{d}t'. \tag{3}$$

$y(t)$ is the normalized response signal and $x(t)$ is a normalized arbitrary input signal. $E(t)$ represents the RTD of the considered micromixer. $y(t)$ and $x(t)$ can be calculated from the measured dataset by Eq. (1). Numerous methods were presented to acquire $E(t)$ when input and response are known [13–15]. Due to the fact that convolution in time domain corresponds to multiplication in frequency or Laplace domain, deconvolution can be carried out in either domain. According to this, the transfer function (which is $E(t)$ in time domain) can be calculated from the measured dataset, e.g. in frequency domain, by

$$E(i\omega) = \frac{\int_0^\infty c_{\mathrm{out}}\,\mathrm{e}^{-i\omega t}\,\mathrm{d}t}{\int_0^\infty c_{\mathrm{in}}\,\mathrm{e}^{-i\omega t}\,\mathrm{d}t}. \tag{4}$$

Inverse transformation of the transfer function from frequency to time domain leads directly to the RTD of the micromixer. Although this method is very fast and straightforward it is not appropriate to the measured RTD curve. Since retransformation of transformed experimental data is always accompanied by a drastic increase of noise, the results are not satisfactory. Nevertheless, this method is useful to verify the results obtained by another deconvolution technique and was used here in this regard. Improvement of the results can be achieved by noise filters and curve smoothing.

Other techniques to obtain the transfer function require the prediction of a model for the RTD. A benefit of this approach is that one gets not only the shape of the curve, but also a model description of the RTD of the measured device. An essential requirement, e.g. for time domain analysis is that an analytical model in closed form can be applied to describe the RTD of the considered microfluidic device adequately. Both models which were used in this work allow time domain analysis. In this process, a model for the unknown $E(t)$ was appointed and the model parameters were successively modified in order to minimize the sum of squares of deviation between the normalized measured response and the predicted curve:

$$\varepsilon = \sum\nolimits_0^{t_{\max}} [y(t) - y_{\mathrm{calc}}(t)]^2. \tag{5}$$

By applying Eq. (3), ε is calculated by numerical integration of

$$\varepsilon = \left[\int_0^\infty \left[y(t) - \int_0^t x(t-t')E(t')\,\mathrm{d}t'\right]\,\mathrm{d}t\right]^2. \tag{6}$$

This integral is best approximated by applying the trapezoidal rule. All calculations in this work were accomplished with the software package Mathematica (Wolfram Research, Champaign, USA). The minimization of ε by means of nonlinear optimization was performed by using the unconstrained quasi-Newton method. This method is useful when numerical operations are involved in the objective function and the derivatives have to be evaluated numerically [16]. Some completely derivative-free methods were also applied. They converge much more slowly and provide only good results when the initial estimation is very good. The quasi-Newton method provides best results even with poor initial estimations.

The approximation of the integral in Eq. (6) has to be done in every iterative step. This is very time-consuming and computationally expensive. Several faster convolution functions using matrix operations are not suitable. In particular, applying such functions to very narrow signals often leads to scaling problems.

The time domain fitting procedure involves numerous steps and numerical transformations. In order to verify the deconvolution result obtained by the time domain fitting procedure, it was compared to a curve obtained by direct deconvolution in Fourier domain (Eq. (4)). In addition to a noise filter an exponential decay of fourth order was applied to the considerably scattered tail part of the curve. An example of a comparison for a measurement at 1.0 mL/min is shown in Fig. 4.

Although the front part of the curve is still very noisy, one can see that the two results are generally in good agreement. Therefore, time domain fitting is suitable for the analysis of the RTD in microfluidic devices. Furthermore,

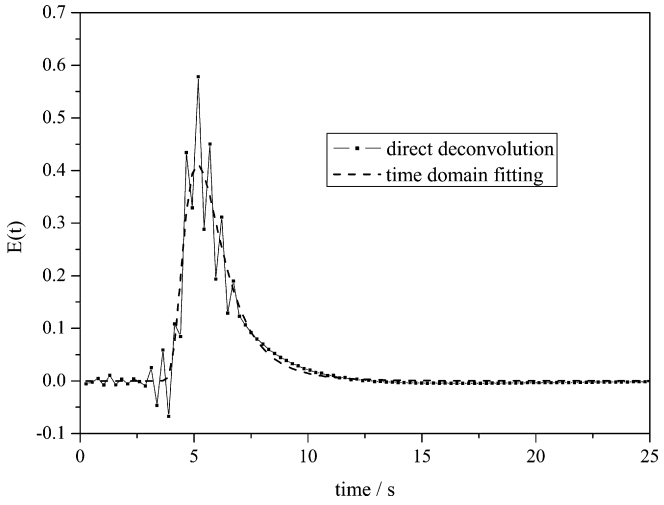

Fig. 4. Comparison of time domain fitting and direct deconvolution for an RTD measurement at 1.0 mL/min, ST-mixer.

it provides much better results than direct deconvolution procedures.

2.3. Modelling

Two fundamentally different models were applied to describe the RTD of the considered split-and-recombine micromixers. The first one is the well-known one-dimensional axial dispersed plug flow model. It takes the form of the one-dimensional diffusion equation with a convective term assuming a mean velocity:

$$\frac{\partial c}{\partial t} = \frac{D_{ax}}{uL}\frac{\partial^2 c}{\partial x^2} - \frac{\partial c}{\partial x}. \tag{7}$$

According to this description, this model applies best to turbulent flow in an empty cylindrical tube. Nevertheless, it is widely used for packed beds and can also be used in a more empirical way to approximately describe a variety of different reactors operating in the laminar flow regime although it does not correspond to the physical model description (e.g. in the present application). The dispersion coefficient D_{ax} comprises all effects causing deviation from plug flow. Hence dispersion, due to convective distribution can be considered to a certain degree. The flow in the considered microfluidic devices is characterised by a velocity gradient due to the laminar flow and a counteracting dispersion due to the split-and-recombine mixing structure. Therefore, the axial dispersed plug flow model can be applied if the micromixers are sufficiently long enough to ensure that dispersion caused by the mixing structure can compensate the spreading of the tracer as a result of the non-uniform velocity profile in laminar flow.

The dimensionless group D_{ax}/uL is usually replaced by the Peclet-number:

$$\frac{1}{Pe} = \frac{D_{ax}}{uL}. \tag{8}$$

Eq. (7) can be solved under "open" boundary conditions [17] leading to

$$E(t) = \sqrt{\frac{Pe}{4\pi\tau t}}\exp\left\{\frac{-Pe\tau}{4t}\left(1-\frac{t}{\tau}\right)^2\right\}. \tag{9}$$

The model is characterised by two parameters, the Peclet number and the mean residence time τ, which can be determined by the previously described fitting procedure.

In the present application "open" boundary conditions were chosen. However, the precise conditions at the boundaries of real equipment cannot usually be exactly defined [3]. The differences between the solutions for different boundary conditions diminish for low values of D_{ax} and therefore high *Pe*-numbers, which is the case in this study.

The axially dispersed plug flow model is based on a physical description of the system. It is the simplest, only one-dimensional form of the convective diffusion equation. As soon as a two-dimensional velocity profile is considered, the equation becomes generally insolvable [18,19]. Due to the strong laminar flow regime prevailing in microfluidics, the appearance of a multidimensional flow profile can in most cases not be disregarded. Therefore, convection-diffusion equations are not suitable to model analytically the RTD behaviour of different microfluidic devices in the whole range of different process conditions.

The second model used in this work is an empirical model which was first published by Ham and Platzer [20]. The model was developed following statistical distributions with main emphasis on allowing certain skewness of the distribution. This is highly useful for applying the model to microfluidic devices concerning the multidimensional flow profiles mentioned above and the resulting asymmetric distributions. The model takes the form:

$$E(t) = \frac{MNt_k^N}{t^{N+1}}\left(1-\frac{t}{t_{max}}\right)^{N-1}\left\{1-\frac{t_k^N}{t^N}\left(1-\frac{t}{t_{max}}\right)^N\right\}^{M-1} \tag{10}$$

with

$$t_k = \frac{t_{min}t_{max}}{t_{max}-t_{min}}. \tag{11}$$

t_{min} and t_{max} are the minimum and maximum residence time and can be estimated by the experimentally obtained RTD curves. Since the curves for laminar systems show significant tailing, this procedure is sometimes problematic in the case of t_{max}. In such a case, it is more reasonable to choose a higher value since for certain skewness the shape of the curve is only weakly influenced. *N* and *M* in Eq. (10) are the model parameters which can be determined by the described fitting procedure. *N* and *M* are pure fitting parameters and correlations between the values of *N* and *M* and the shape of the curve cannot be found due to the complex composition of the parameters in the model. A detailed study on the behaviour of this model can be found in [20].

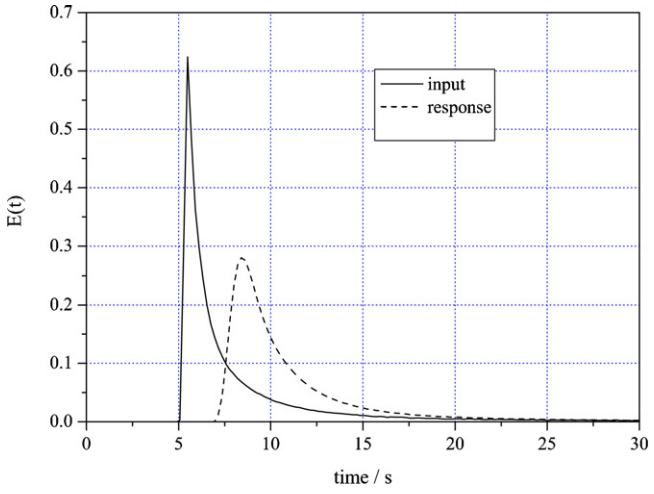

Fig. 5. Normalized density distribution curves for the ST-mixer from a measurement at 1.5 mL/min.

3. Results and discussion

The RTD of the three different micromixers were measured at flow rates between 0.5 and 2.0 mL/min. The normalized density distribution functions for all experimentally obtained input and response curves were calculated by Eq. (1).

As an example, the RTD of one measurement (ST-mixer at 1.5 mL/min) is shown in Fig. 5.

The curve of the input signal shows a nearly vertical rise at minimum residence time and a decreasing slope at lower flow rates. The strong influence of convective dispersion due to the laminar flow profile is evident. Consequently, a pure convection model derived from the parabolic velocity profile was applied to the input signal, in order to use the calculated input signal for the convolution in the fitting procedure instead of the measured input. The aim was to achieve faster calculations and easier measurements since only the response signal would be necessary to measure. Unfortunately, the deviation from the model was too strong. Therefore, it is obligatory to measure also the input signal and use it for the modelling.

A comparison of first modelling results obtained for the ST-mixer at maximum and minimum flow rate is shown in Fig. 6.

Both the axially dispersed plug flow model and the empirical model were applied. Each diagram shows three curves. The curves labelled with "fit" are the convolution products of the input signal and the predicted model fitted to the response signal, which is labelled with "response". Hence, the predicted model represents the RTD of the isolated microfluidic device. For the higher flow rate both models fit very well. The deviation between the calculated convolution product and the measured response, by means of the sum of squares of deviation ε is 0.00724 for the dispersion model and 0.00172 for the empirical model. The better value for the empirical model is due to the asymmetry which enables a steeper rise at the front part of the curve and a smoother tail. The difference in the quality of the fit increases at lower flow rates. At a flow rate of 0.5 mL/min the front part and the tail part cannot be predicted satisfactorily with the dispersion model whereas the empirical model matches very well. The difference in the sum of squares of deviation is nearly one order of magnitude and counts 0.00028 for the empirical model and 0.00200 for the dispersion model.

The modelling results for all three considered micromixers at all flow rates are shown in Fig. 7. For a better comparability the same model was applied to all measurements. Since it can cover the whole range more satisfactorily, the empirical model was used. It is also convenient to use the dimensionless time:

$$\Theta = \frac{t}{\tau} \tag{12}$$

for a better comparability of measurements at different process parameters.

Generally, all micromixers show similar behaviour. At a flow rate of 0.5 mL/min the distributions are broader and the tailing and the skewness is more distinctive. With higher flow rate the RTD becomes narrower and more symmetric.

The mixing in split-and-recombine mixers is based on sequential multilamination. After m split-and-recombine steps 2^m liquid layers could be formed. Of course, this is a theoretical examination and is only valid for a limited extend since it depends strongly on the geometry of the microfluidic structure. For example, splitting, reorganisation and recombination is very well defined for the G-shaped mixer, whereas mainly splitting and only poor reorganisation takes place in the ST-mixer. However, it is nowadays known that in such micromixers multilamination is always superimposed by secondary flows causing chaotic advection and enhancing radial mixing [6,7]. Since the generation of secondary flows is highly dependent on the Reynolds number, the radial mixing increases at higher flow rates for all considered micromixers which can be confirmed by the narrower RTD.

Apart from the visual examination, determination of the central moments [19,20] provides an opportunity to study the modelled distribution curves. As already mentioned the mean residence time τ can be calculated by the first statistical moment in analogy to probability theory. The second central moment:

$$\sigma(t)^2 = \int_0^\infty (t-\tau)^2 E(t)\,\mathrm{d}t \tag{13}$$

gives the variance which can be transformed to the dimensionless form:

$$\sigma(\Theta)^2 = \frac{\sigma(t)^2}{\tau^2}. \tag{14}$$

The variance is a measure for the "width" of a distribution. With regard to RTD, narrower distributions are aspired and therefore lower variance.

Another useful parameter for the present application is the third central moment which is known as the skewness of a distribution:

$$s = \frac{\int_0^\infty (t-\tau)^2 E(t)\,\mathrm{d}t}{\sigma(\Theta)^{3/2}}. \tag{15}$$

The shape of the RTD in the considered micromixers at the applied flow rates varies from very symmetric, when good radial mixing is achieved to very asymmetric when radial mixing is

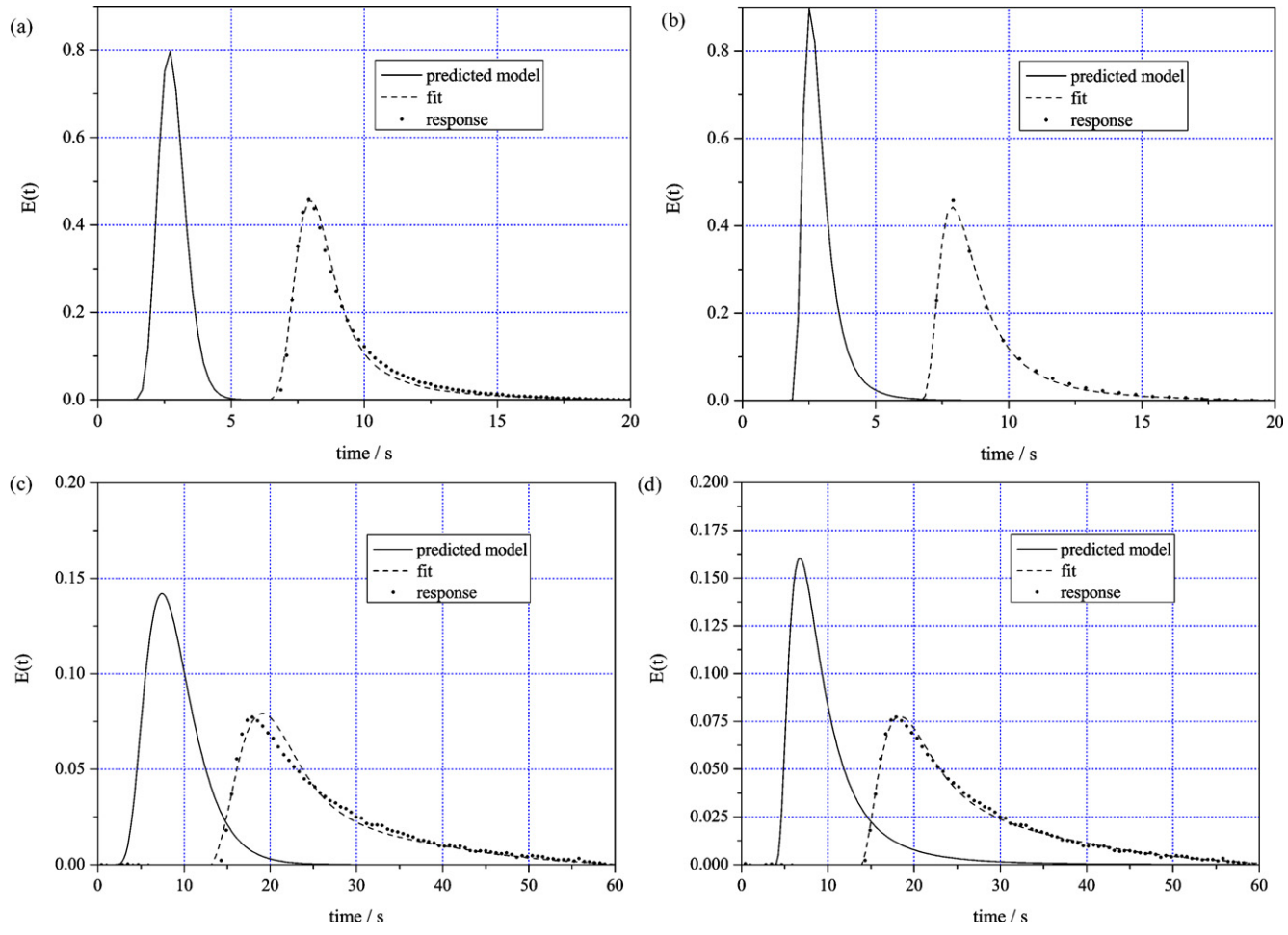

Fig. 6. (a) Modelling result for the ST-mixer at 2.0 mL/min with dispersion model. (b) Modelling result for the ST-mixer at 2.0 mL/min with empirical model. (c) Modelling result for the ST-mixer at 0.5 mL/min with dispersion model. (d) Modelling result for the ST-mixer at 0.5 mL/min with empirical model.

very poor and the influence of the parabolic flow profile is prevailing. The skewness measures zero for symmetric distributions (e.g. axially dispersed plug flow at high *Pe* numbers) and is going towards infinity for pure laminar flow in a tube. Since the measurements were performed at a pure laminar regime, decrease of the skewness can provide an indication of a better radial mixing.

Variance, skewness and corresponding Reynolds numbers for all obtained distribution curves are listed in Table 1. The moments were calculated by numerical integration (Eq. (13)–(15)) of the RTD-curves which were obtained by the fitting procedure. The Reynolds number was calculated by

$$Re = \frac{u d_h}{\nu} \tag{16}$$

with the hydraulic diameter as characteristic length.

The ST-mixer shows the widest range of different distributions which can be seen visually in Fig. 7 and also by means of the values in Table 1. At 0.5 mL/min the ST-mixer has the highest variance of all micromixers. It improves considerably at higher flow rates, resulting in a very low variance at 2.0 mL/min. As expected, the skewness decreases as well and has generally lower values than calculated for the other micromixers. This

Table 1
Comparison of variance and skewness of the distribution curves with corresponding Reynolds numbers for the considered micromixers at different flow rates

Flow rate (mL/min)	Variance, $\sigma(\Theta)^2$	Skewness, s	*Re* number
ST-mixer			
0.5	0.30	3.18	5
1.0	0.10	3.13	11
1.5	0.08	3.06	17
2.0	0.06	2.63	23
G-shaped mixer			
0.5	0.22	3.13	3
1.0	0.16	3.43	6
1.5	0.11	3.42	9
2.0	0.09	3.00	12
Statmix 6			
0.5	0.25	5.60	20
1.0	0.12	4.00	40
1.5	0.10	3.64	63
2.0	0.07	3.11	83

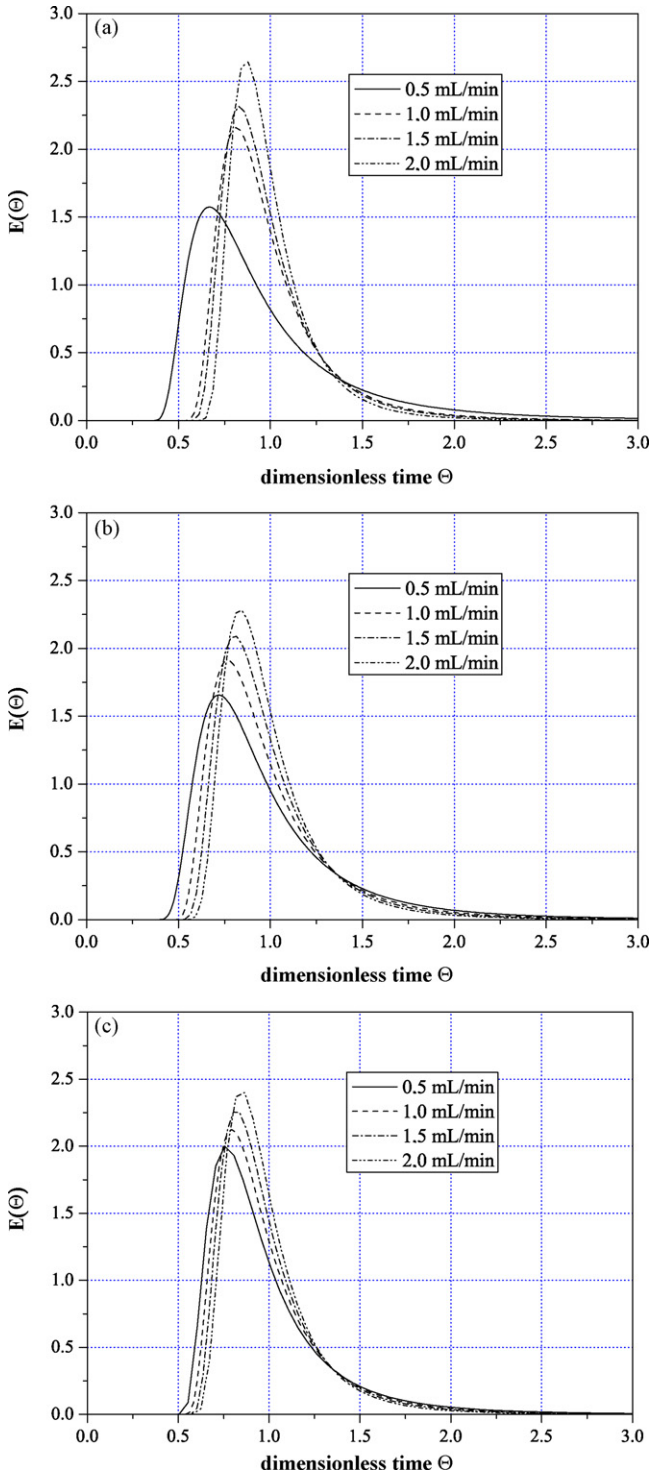

Fig. 7. RTD for the three investigated micromixers obtained by the modelling technique: (a) ST-mixer, (b) G-shaped mixer, (c) Statmix 6.

behaviour is explained by the specific mixing structure that provides a high degree of chaotic advection. However, regarding the fact, that the *Re* numbers are very low in the ST-mixer, it shows very good mixing performance, mainly at flow rates higher than 1.0 mL/min.

Due to the parallelisation of microchannels in the G-shaped mixer the *Re* numbers are lower although the channels are smaller in diameter. Nevertheless, the variances are quite low and in a narrow range. The values for the skewness are a bit higher than those obtained for the ST-mixer. This can be due to less developed secondary flows in the more ordered split-and-recombine structure. A stronger tailing can also be caused by the parallelisation and thus a slightly inhomogeneous flow splitting. However, the parallelisation in the G-shaped mixer performs very well since the variances and skewness are only slightly higher than for the one-channel ST-mixer. The efficiency of the trapezoidal inlet and outlet-structures was also proved in previous works [10,11].

The Statmix 6 mixer provides the highest *Re* numbers at the considered flow rates. The variances are in the same range as for the G-shaped mixer. The values for the skewness are somewhat higher. Again, this is explained by less developed secondary flows and thus stronger generation of non-uniform flow profiles. In general, the other two micromixers are somewhat more efficient by means of residence time distribution since the distributions are narrower and more symmetric at lower *Re* numbers.

4. Conclusions

An experimental method was developed for the measurement of the RTD in various micromixers. Since it is not possible to obtain the actual RTD within the microfluidic devices directly from the measured data, different possibilities for the required deconvolution were applied and discussed. It was shown that time domain fitting by predicting an algebraic model for the RTD of the micromixers leads to the best results.

The widely used axial dispersed plug flow model was used to fit the measured RTD data. It was shown that the results with this model applied to the considered micromixers are only satisfactory for higher flow rates (*Re* numbers) when the distributions become more symmetric. A wider flow range can be made available by the use of empirical models which allow more asymmetric distributions.

Three different micromixers based on split-and-recombine mixing structures were characterised by means of RTD at different flow rates. The empirical model could be used in the whole considered range, which allows a closer examination of the mixing performance and integral flow behaviour of micromixers and other microfluidic devices.

Acknowledgements

We are grateful to Prof. Michael Köhler from the Technical University Ilmenau for fruitful discussions. Skilful assistance by Klaus Huber is also gratefully acknowledged.

References

[1] M. Guenther, S. Schneider, J. Wagner, R. Gorges, Th. Henkel, M. Kielpinski, J. Albert, R. Bierbaum, J.M. Koehler, Characterisation of residence time and residence time distribution in chip reactors with modular arrangements by integrated optical detection, Chem. Eng. J. 101 (2004) 373–378.

[2] F. Trachsel, A. Guenther, S. Khan, K.F. Jensen, Measurement of residence time distribution in microfluidic systems, Chem. Eng. Sci. 60 (2005) 5729–5737.

[3] K.B. Bischoff, O. Levenspiel, Fluid dispersion-generalization and comparisopn of mathematical models, Chem. Eng. Sci. 17 (1962) 245–255.
[4] T. Korenaga, F. Shen, T. Takahashi, An experimental study of the dispersion in laminar tube flow, AIChE J. 35 (1989) 1395–1398.
[5] D. Bošković, S. Löbbecke, The use of input–response measurements as a basis for modeling the residence time distribution of microreactors, in: Proceedings of the 8th International Conference on Microreaction Technology (IMRET 8), Atlanta, USA, 2005.
[6] V. Hessel, H. Loewe, F. Schönfeld, Micromixers—a review on passive and active mixing principles, Chem. Eng. Sci. 60 (2005) 2479–2501.
[7] N.T. Nguyen, Z. Wu, Micromixers—a review, J. Micromech. Microeng. 15 (2005) R1–R16.
[8] F. Schoenfeld, V. Hessel, C. Hoffmann, An optimised split-and-recombine micromixer with uniform "chaotic" mixing, Lab Chip 4 (2004) 65–69.
[9] S. Panic, S. Loebbecke, T. Tuercke, J. Antes, D. Bošković, Experimental approaches to a better understanding of mixing performance of microfluidic devices, Chem. Eng. J. 101 (2004) 409–419.
[10] J.M. Commenge, L. Falk, J.P. Corriou, M. Matlosz, Optimal design for flow uniformity in microchannel reactors, in: Proceedings of the Fourth International Conference on Microreaction Technology (IMRET 4), Atlanta, USA, 2000.
[11] W. Ferstl, S. Löbbecke, J. Antes, H. Krause, M. Grund, M. Häberl, H. Muntermann, D. Schmalz, J. Hassel, A. Lohf, A. Steckenborn, T. Bayer, M. Kinzl, I. Leipprand, Development of an automated microreaction system with integrated sensorics for process screening and production, Chem. Eng. J. 101 (2004) 431.
[12] T. Kirner, J. Albert, M. Guenther, G. Mayer, K. Reinhäckel, J.M. Koehler, Static micromixers for modular chip reactor arrangements in two-step reactions and photochemical activated processes, Chem. Eng. J. 101 (2004) 65–74.
[13] M.L. Michelsen, A least squares method for residence time distribution analysis, Chem. Eng. J. 4 (1972) 171–179.
[14] A.D. Martin, Interpretation of residence time distribution data, Chem. Eng. Sci. 55 (2000) 5907–5917.
[15] M.A. Fahim, N. Wakao, Parameter estimation from tracer response measurements, Chem. Eng. J. 25 (1982) 1–8.
[16] J. Nocedal, S.J. Wright, Numerical Optimization, Springer, New York, 1999.
[17] O. Levenspiel, W.K. Smith, Notes on the diffusion-type model for the longitudinal mixing of fluids in flow, Chem. Eng. Sci. 6 (1957) 227–233.
[18] C.Y. Wen, L.T. Fan, Models for Flow Systems and Chemical Reactors, Dekker, New York, 1975.
[19] E.B. Naumann, B.A. Buffham, Mixing in Continuous Flow Systems, Wiley, New York, 1983.
[20] J.H. Ham, B. Platzer, Semi-empirical equations for residence time distributions in disperse systems. Part 1. Continuous phase, Chem. Eng. Technol. 11 (2004) 1172–1178.